Communication

Carbon–Hydrogen Bond Activation: Two, Three, or More Mechanisms?

Benjamin Alan Vastine, and Michael B. Hall

J. Am. Chem. Soc., **2007**, 129 (40), 12068-12069• DOI: 10.1021/ja074518f • Publication Date (Web): 14 September 2007

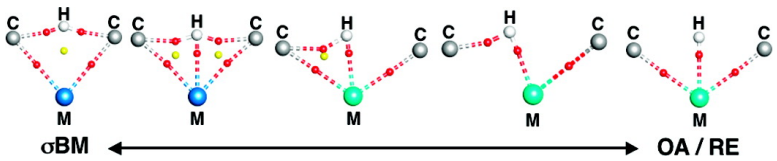

More About This Article

Additional resources and features associated with this article are available within the HTML version:

- Supporting Information
- Links to the 6 articles that cite this article, as of the time of this article download
- Access to high resolution figures
- Links to articles and content related to this article
- Copyright permission to reproduce figures and/or text from this article

View the Full Text HTML

J|A|C|S
COMMUNICATIONS

Published on Web 09/14/2007

Carbon−Hydrogen Bond Activation: Two, Three, or More Mechanisms?

Benjamin Alan Vastine and Michael B. Hall*

Department of Chemistry, Texas A&M University, P.O. Box 30012, College Station, Texas 77841-3255

Received June 20, 2007; E-mail: hall@science.tamu.edu

Carbon−hydrogen bond activation, a critically important step in a variety of reactions, has received considerable attention.[1] For the special case of hydrogen transfer (HT) between R′−H and M−R, there are two well-established mechanisms (Scheme 1): (a) σ-bond metathesis (σBM)[2] and (b) oxidative addition/reductive elimination (OA/RE).[3] Historically, the midpoint in the reaction coordinate for σBM has been characterized as a single four-centered transition state (TS) with a small R′−M−R angle and a nonbonding M−H distance, while the midpoint for the OA/RE mechanism has been characterized as an intermediate (INT) with a higher formal oxidation state ($n + 2$), a large R′−M−R angle, and a M−H bond. Recently, several groups have suggested alternative mechanisms that appear to be in between these extremes.[4−7] We termed our alternative mechanism metal-assisted σ-bond metathesis (MAσBM);[4] Lin and co-workers termed theirs oxidatively added transition state (OATS);[5] Oxgaard et al. termed theirs oxidative hydrogen migration (OHM),[6] and Perutz et al. termed theirs σ-complex assisted metathesis (σ-CAM).[7] The identification of these different mechanisms has typically been only through comparison of computed geometric parameters. Here, we analyze the reaction coordinate midpoint (INTs or TSs) of these mechanisms with Bader's atoms in molecules (AIM) analysis.[8] The midpoints of the alternative mechanisms are all TSs that directly connect reactant and product. Through this analysis, we show that mechanisms can be unambiguously differentiated on the basis of their AIM bonding patterns.

All optimized geometries and analytical frequencies were calculated in Gaussian 03[9] at the B3LYP/DZP[10] level of theory. The character (INTs vs TSs) of the species was identified through the frequency calculations. AIM2000[11] was used to analyze the electron density, its gradient field, and its Laplacian; bond (B) and ring (R) critical points (CP) in the gradient field were located through this analysis.[12] A BCP is essential for a direct interaction between atoms and is symbolized by a red dot in the AIM representations. A RCP is symbolized by a yellow dot. All 3D molecular and AIM representations were made with JIMP2 visualization software.[13] The dashed lines that connect critical points in the following figures are approximate bond paths.

The σBM and OA/RE mechanisms, the two "classic" mechanisms for HT, have been theoretically investigated by methane addition to $[Cp_2ScCH_3]$ (Cp = η^5-C_5H_5) and to $[Cp^*Ir(PMe_3)(C'H_3)]^+$ (Cp* = η^5-$C_5(CH_3)_5$), respectively, as models closely related to the experimental systems.[2,3,14] Figure 1 shows the optimized geometric parameters, which agree well with published data, and CPs of the σBM TS, $[Cp_2Sc(CH_3)_2H]^‡$ (**1**), the OA/RE INT, $[Cp^*Ir(PMe_3)(CH_3)(C'H_3)H]^+$ (**2**), and the OA/RE TS, $[[Cp^*Ir(PMe_3)(CH_4)(C'H_3)]^+]^‡$ (**3**). Geometrically, **1** has a long Sc−H distance and a small C−Sc−C angle, whereas **2** has a short Ir−H distance and a large C−Ir−C′ angle. In the AIM analysis, **1** is characterized by two Sc−C BCPs, two C−H BCPs, and a RCP at the center of the four-centered TS, while **2** is characterized by Ir−C, Ir−C′, and Ir−H BCPs. As expected for this INT (**2**), no interactions between the hydride and pendent methyl ligands such as those in **1** are found. The TS for OA/RE, **3**, is responsible for C−H cleavage leading to formation of **2**. At the TS's optimized geometry, BCPs are found for the "breaking" C−H bond and "forming" Ir−H bond, but not for the "forming" Ir−C bond.

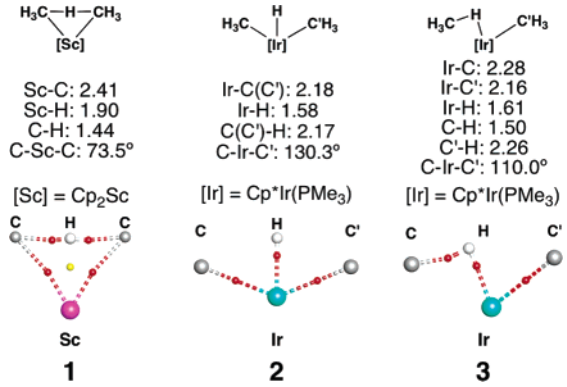

Figure 1. B3LYP/DZP optimized geometric parameters and AIM critical points for **1**, **2**, and **3**. Distances are given in angstroms.

Scheme 1

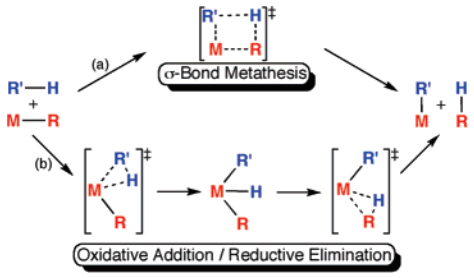

Among the systems proposed to proceed by one of the new mechanisms is the asymmetric HT that occurs between C^{sp3} and C^{sp2} atoms in the Ir^V, seven-coordinate TS $[(acac)_2Ir(C_2{}^{sp3}H_4Ph)(C_6{}^{sp2}H_5)H]^‡$ (**4**) in the reaction of the alkane with $(acac)_2IrPh$.[6] Geometrically, TS **4** has an Ir−H bond length comparable to **2**; the C^{sp3}− and C^{sp2}−H interactions of 1.68 and 1.93 Å, respectively, are shorter than those of **2** but longer than those of **1**, and the C−Ir−C angle is intermediate to those of **1** and **2**. In the AIM analysis, **4** is characterized by Ir−C^{sp3}, Ir−C^{sp2}, Ir−H, and C^{sp3}−H BCPs with a RCP inside the Ir−C^{sp3}−H coordinates. Interestingly, in this TS, the transferring hydrogen is shown to interact with the metal center and only one of the pendent ligands. The geometric parameters and AIM representation of **4** are shown in Figure 2.

In order to understand **4** more thoroughly, we examined analogous reactions which proceed through symmetric HT between and C^{sp3} and C^{sp2} atoms in $[(acac)_2Ir(Me)_2H]$ (**5**) and $[(acac)_2Ir(Ph)_2H]^‡$ (**6**), respectively (Figure 2). HT between two methyl ligands proceeds through **5**, which is a C_2 symmetric, Ir^V, seven-coordinate INT, while a similar reaction between two phenyl ligands proceeds through **6**, which is a C_2 symmetric, seven-coordinate TS. In both **5** and **6**, the Ir−C and Ir−H distances are similar to those

10.1021/ja074518f CCC: $37.00

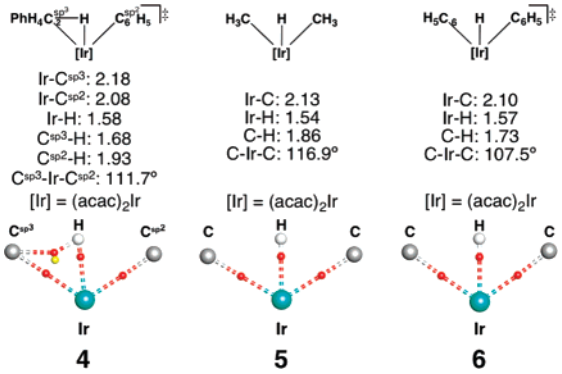

Figure 2. B3LYP/DZP optimized geometric parameters and AIM critical points for **4**, **5**, and **6**. Distances are given in angstroms.

Table 1. Geometric Parameters for Osmium and Platinum Complexes[a]

	[(acac)$_2$Os(X)$_2$H]$^-$		[(acac)$_2$Pt(X)$_2$H]$^+$	
	Me (**7**)	Ph (**8**)	Me (**9**)	Ph (**10**)
M−H	1.58	1.59	1.63	1.92
M−C	2.15	2.11	2.17	2.13
C−H	1.99	1.91	1.56	1.42
C−M−C	124.5	120.3	91.6	81.6
midpoint species	INT	INT	TS	TS

[a] Distances in angstroms, angles in degrees.

in **2** and **4**, but the C−M−C angles are smaller than the angle of **2** and comparable to that of **4**. Interestingly, **5** and **6** are characterized by Ir−C and Ir−H BCPs only; even in TS **6**, no C−H interactions were found. Note that in **4** the C−H BCP not found in **5** or **6** is close to the RCP; the coalescence of the two CPs would result in their annihilation, and then **4** would resemble intermediate **5** or TS **6**.

To explore the full range of possible mechanisms for HT, the iridium center of **5** and **6** was replaced to produce the isoelectronic osmium and platinum species ([(acac)$_2$Os(X)$_2$H]$^-$, X = Me (**7**), Ph (**8**); [(acac)$_2$Pt(X)$_2$H]$^+$, X = Me (**9**), Ph (**10**)). The optimized geometric parameters are found in Table 1. For osmium, both **7** and **8** are INTs with M−H distances similar to the other INTs studied, but with larger C−M−C angles and longer C−H distances. On the other hand, both platinum species are TSs with longer Pt−H distances and smaller C−Pt−C angles. Compared to **9**, the smaller C−Pt−C angle in **10** is accompanied by a longer Pt−H distance. In the AIM analysis, the osmium INTs (**7**, **8**) are characterized by the same CPs as the other INTs (**2**, **5**); however, the two platinum TSs are characterized differently. For **9**, two Pt−C, two C−H, and one Pt−H BCPs were found with one RCP inside of each Pt−H−C coordinates. TS **9** is unique because the transferring hydrogen is shown to interact with *both* pendent ligands *and* the metal center (shown as **B** in Figure 3). TS **10** is characterized by the same CPs as **1**, as the Pt−H distance is too great for an interaction (shown as **A** in Figure 3).

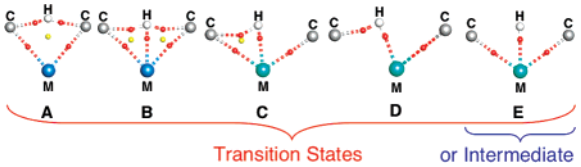

Figure 3. Spectrum of mechanisms for metal-mediated hydrogen transfer.

This study provides a spectrum of mechanisms for metal-mediated HT that can be resolved by AIM analysis. The resolution of this spectrum is shown in Figure 3 with suggested assignments of **A** = σBM (**1**, **10**); **B** = MAσBM (**9**); **C** = OATS/σ-CAM (**4**); **D** = OA/RE TS (**3**); and **E** = OHM TS or OA/RE INT (**2**, **5**−**8**).

Acknowledgment. This work was supported by grants from the NSF (CHE-0518074 and DMS-0216275) and The Welch Foundation (A0648).

Supporting Information Available: All optimized geometries and AIM data for models considered in this report, an explanation of AIM analysis, and optimized geometric parameters for species **7**, **8**, **9**, and **10**. This material is available free of charge via the Internet at http://pubs.acs.org.

References

(1) (a) Godula, K.; Sames, D. *Science* **2007**, *312*, 67−72. (b) Lersch, M.; Tilset, M. *Chem. Rev.* **2005**, *105*, 2471−2526. (c) *Activation and Functionalization of C−H Bonds*; Goldberg, K. I., Goldman, A. S., Eds.; Oxford University Press: Washington, DC, 2004.
(2) (a) Watson, P. L. *J. Am. Chem. Soc.* **1983**, *105*, 6491−6493. (b) Watson, P. L.; Parshall, G. W. *Acc. Chem. Res.* **1985**, *18*, 51−56.
(3) (a) Arndtsen, B. A.; Bergman, R. G. *Science* **1995**, *270*, 1970. (b) Crabtree, R. H. *Chem. Rev.* **1985**, *85*, 245−269.
(4) (a) Webster, C. E.; Fan, Y.; Hall, M. B.; Kunz, D. Hartwig, J. F. *J. Am. Chem. Soc.* **2003**, *125*, 858−859. (b) Hartwig, J. F.; Cook, K. S.; Hapke, M.; Incarvito, C. D.; Fan, Y.; Webster, C. E.; Hall, M. B. *J. Am. Chem. Soc.* **2005**, *127*, 2538−2552.
(5) (a) Ng, S. M.; Lam, W. H.; Mak, C. C.; Tsang, C. W.; Jia, G.; Lin, Z.; Lau, C. P. *Organometallics* **2003**, *22*, 641−651. (b) Lam, W. H.; Jia, G.; Lin, Z.; Lau, C. P.; Eisenstein, O. *Chem.—Eur. J.* **2003**, *9*, 2775−2782. (c) Lin, Z. *Coord. Chem. Rev.* **2007**, doi:10.1016/j.ccr.2006.11.006.
(6) (a) Oxgaard, J.; Muller, R. P.; Goddard, W. A., III; Periana, R. A. *J. Am. Chem. Soc.* **2004**, *126*, 352−363. (b) Oxgaard, J.; Periana, R. A.; Goddard, W. A., III. *J. Am. Chem. Soc.* **2004**, *126*, 11658−11665.
(7) Perutz, R. N.; Sabo-Etienne, S. *Angew. Chem., Int. Ed.* **2007**, *46*, 2578−2592.
(8) Bader, R. F. W. *Atoms in Molecules: A Quantum Theory*; Oxford: New York, 1990.
(9) Frisch, M. J.; et al. *Gaussian 03*; see Supporting Information for full citation.
(10) (a) Becke, A. D. *J. Chem. Phys.* **1993**, *98*, 5648−5652. (b) Lee, C.; Yang, W.; Parr, R. G. *Phys. Rev. B: Condens. Matter Mater. Phys.* **1988**, *37*, 785−789. (c) For a listing of basis sets used in this study, see the Supporting Information.
(11) *AIM2000*; Biegler-König, F. W.; Schönbohm, J.; Bayles, D. *J. Comput. Chem.* **2001**, *22*, 545 (http://www.aim2000.de).
(12) For a discussion of AIM in greater detail, see the Supporting Information.
(13) (a) Manson, J.; Webster, C. E.; Pérez, L. M.; Hall, M. B. *JIMP Development Version 0.1 (built for Windows PC and Redhat Linux 7.3)*; Department of Chemistry, Texas A&M University: College Station, TX, 2003 (available @ http://www.chem.tamu.edu/jimp2/index.html). (b) Hall, M. B.; Fenske, R. F. *Inorg. Chem.* **1972**, *11*, 768−779.
(14) For σBM, see: Ziegler, T.; Folga, E.; Berces, A. *J. Am. Chem. Soc.* **1993**, *115*, 636−646. For OA/RE, see: (a) Strout, D. L.; Zarić, S.; Niu, S.; Hall, M. B. *J. Am. Chem. Soc.* **1996**, *118*, 6068−6069. (b) Niu, S.; Hall, M. B. *J. Am. Chem. Soc.* **1998**, *120*, 6169−6170. (c) Niu, S.; Hall, M. B. *Chem. Rev.* **2000**, *100*, 353−406.

JA074518F